



Design, Synthesis, Anticancer Activity and Molecular Docking of New 1,2,3-Triazole combined Glucosides with coumarin

Ruaa Wassim Adam^{1*}, Ezzat Hussein Zimam²

^{1,2}Department of Chemistry, Faculty of Science, University of Kufa, Najaf, Iraq

*Corresponding author: Ruaa Wassim Adam, Department of Chemistry, Faculty of Science, University of Kufa, Najaf, Iraq, Email: ruaaw.abdulfadhil@uo.kufa.iq

Submitted: 22 February 2023; Accepted: 17 March 2023; Published: 01 April 2023

ABSTRACT

The synthetic strategy for the preparation of the targeted glycosides involved two different pathways to obtain two types of hybrid compounds; the first represents new 1,2,3-triazole derivative in the 6-carbon glucopyranose, and the other is a new glycoside of 4-hydroxy coumarin bases. The starting derivative 1 prepared by reaction of 6-azide glucopyranose and 2 ethylene azide-2,3,4,6-tetraacetate- β -D- glucopyranoside with propargyl 4-hydroxy coumarin under click conditions. The cytotoxicity potentials of glucosides derivatives were evaluated by MTT assay against liver cancer primary tissue culture, which appear that derivatives exhibited selective cytotoxicity against liver cancer cells isolated from Iraqi patients with inhibitory concentration (IC₅₀) 106.81 μ g/ml. Docking simulation studies were performed to check the binding patterns of the synthesized compounds. Enzyme inhibition assay studies were also conducted for the epidermal growth factor receptor (EGFR), and the results explained the activity of a number of derivatives.

Keywords: Carbohydrate, 4-hydroxy coumarin, Click chemistry, 1,2,3-triazole

INTRODUCTION

Heterocyclic moieties bearing nitrogen atoms, such as 1,3,4-thiadiazole and 1,2,3-triazole, play a critical role in medicinal chemistry and are associated with different pharmaceutical properties, such as anticancer, antimicrobial, antidiabetic, anti-inflammatory and antihypertensive¹. Carbohydrates are ubiquitously present in a wide range of plants, animals, and micro organisms. Their irreplaceable biological roles have been well established. To date, a large number of carbohydrate-containing drugs have been approved worldwide. However, the development of carbohydrate-containing drugs seems to have slowed down in recent years. Of more than 200 drugs that have been approved during 2015–2020,

only nine are small-molecule carbohydrate-containing drugs². Carbohydrates are involved in an extensive range of processes, such as signaling, cell-cell communication, and molecular and cellular targeting. Further biological processes, such as blood clotting and fertilization, require carbohydrates, and the biological implications of these compounds are strongly related to diseases such as cancer, diabetes, and inflammatory processes³. Coumarin, of artificial and natural origin, is a broad family of cyclic heterocyclic compounds that contain a benzo-a-pyrone group. Coumarin is widely distributed on plants⁴. Coumarins are extensively found in the field of biology, medicine, and polymer sciences. The most well-known and important coumarin is “warfarin”,

which is prescribed in low doses as a blood thinner. Numerous coumarins are used as a drug in contemporary and recent medicine⁵. 4-Hydroxycoumarins are among the most important coumarin derivatives, because they contain a wide range of biological activities. They can be anticoagulant, antibacterial, anti-HIV active, and anti-tumoral. The nucleus of 4-hydroxycoumarin is very susceptible to electrophilic substitution, so they are very easy synthesized and substituted by other functional groups to enhance their biological activities⁶. Click chemistry is a synthesis philosophy that was conceived, primarily, to help catalyse the discovery and development of reliable and robust reactions⁷. The basic procedure below describes the ligation of a functional (“cargo”) azide to a biomolecule-alkyne. It can be used equally well in the reversed sense (biomolecule azide + cargo-alkyne), and the cargo can also be a biomolecule⁸. Diels–Alder reactions and copper(I)-catalyzed azide–alkyne cycloaddition (CuAAC) reactions. Among the various click reactions, the most successful and extensively applied reaction in the construction of complex polymer⁹. Click Chemistry Copper-catalyzed azide alkyne cycloaddition (CuAAC) is a type of Huisgen 1,3-dipolar cycloaddition based on the formation of 1,4-disubstituted 1,2,3- triazoles between a terminal alkyne and an aliphatic azide in the presence of copper, and is classified as a ‘click reaction’. Click chemistry promotes the use of organic reactions that allow the connection of two molecular building blocks in a facile, selective, high-yielding reaction under mild reaction conditions with few or no byproducts¹⁰. 1,2,3-triazoles are among the most common amide bond isosteres. In fact, despite some differences concerning the overall dipolar moment and distance between the substituents, their structural features allow a good overlap with amide-binding moiety¹¹.

2. EXPERIMENTAL

2.1. General

¹H and ¹³C NMR spectra in DMSO-d₆ were obtained on Bruker spectrometer (300MHz for ¹H-NMR and 75 MHz for ¹³C-NMR, respectively), Shahid Beheshti University/Iran.

FT-IR spectra were recorded using Fourier transform infrared Alpha-Broker (Germany) infrared spectrophotometer, Department of Chemistry, Faculty of Science, University of Kufa. The values of ppm, also known as chemical shifts, are provided in relation to TMS, which serves as a reference standard. The coupling constants, denoted by the J values, are expressed in hertz. TLC, employing aluminum silica gel 60 F245, infrared spectroscopy, nuclear magnetic resonance (¹H and ¹³C), and elemental analyses were used to monitor and direct the progression of the reaction.

*1-Synthesis of ((2R,3S,4S,5R,6R)-3,4,5-trihydroxy-6-methoxytetra hydro-2H-pyran-2-yl) methyl 4-methylbenzenesulfonate (a1)*¹²

adding 1.2 equiv. of TsCl in a solution of 1equiv.of methyl β-D-glucopyranoside in dry pyridine at 0 °C. The mixture was then gradually warmed up to room temperature. The reactions were monitored by TLC, mass spectrometry and H1NMR, between 2 and 24 hours of stirring. It is evident that, de- spite the use of an excess of TsCl. the conversion remains limited and unreacted glucose was still present in a significant amount.

Chemical Formula: C₁₄H₂₀O₈S, 81% yield; FTIR, ν (cm⁻¹) 3316, 3068, 2910, 1624.

1-Synthesis Of 2-Bromoethyl-2,3,4,6-tetra-O-acetyl-β-D-glucopyranoside or (2r,3r,4s,5r,6r)-2-(Acetoxymethyl)-6-(2-Bromoethoxy) Tetrahydro-2h-Pyran-3,4,5-Triyl Triacetate (b2)¹³.

Penta-O-acetyl-β-D-glucopyranose (b1) (62.45 g, 0.16 mol) and 2-bromoethanol (13.9 mL, 0.19 mol) were dissolved in dry CH₂Cl₂ (250 mL) in the dark and cooled to 0°C. BF₃·Et₂O (100 mL, 0.81 mol) was then slowly added. The mixture was then stirred at 0°C for 3 h and for 20 h at room temperature. After completion of the reaction, CH₂Cl₂ (50 mL) was added to the mixture, which was then poured into cold water (250 mL) with vigorous stirring. The organic layer was separated and washed repeatedly with water and saturated sodium bicarbonate. The organic phase was dried over anhydrous Na₂SO₄ and concentrated on a rotary evaporator. The

resulting residue was purified by flash chromatography (stationary phase: silica gel; mobile phase: 2% methanol in CH₂Cl₂). The product was a white crystalline solid, yield 37.01 g (50%).

3- General procedure for the protection of hydroxyl group in glucopyranoside a2 & b1¹⁴.

In order to prepare O-acetyl methyl -D-glucopyranoside, acetic anhydride was added to a chilled mixture of a1&b (1.0 g) and pyridine (50 mL) (15 mL). The mixture was agitated all night before being transferred to an EtOAc-filled separating funnel (50 mL). The mixture was refined further by crystallization in EtOAc/hexane, yielding virtually quantifiable amounts of 2.263 g of O-acetyl methyl-D-glucopyranoside, after being washed with 2 N HCl, saturated NaHCO₃, and brine.

4- Synthesis of (ethynyloxy)-2H-chromen-2-one (a4)¹⁵.

(0.01 mol) from 4-hydroxy coumarin was dissolved in acetone (30 ml), then (1g) potassium carbonate K₂CO₃ was added to the reaction solution and stirred for 15 min before the propargyl bromide 1.5 ml was added. the progress of reaction was monitored by using TLC, stirring continued until the reaction complete, followed by adding of 40 ml D.W and two organic and aqueous phases were separated. the organic phase was dried by adding (Na₂SO₄) anhydrous sodium sulfate and then separated by filtration. finally organic phase was evaporated.

Chemical Formula: C₁₂H₈O₃, 88% Yield, The IR spectrum showed the absence of -OH absorption band of starting hydroxy coumarin and displayed a weak absorption in the region 2140 cm⁻¹ for the acetylenic moiety.

4- General procedure for the synthesis of azide sugars a3 & b3¹⁶.

(0.01mol) from compound (a2&b2) was dissolve in (15 ml) from DMF and add of 0.01 mol from sodium azide reflex the reaction at 120 CO, the reaction course was followed by TLC ethyl acetate: hexane as eluent. The crude material was

purified by column chromatography ethyl acetate: hexane and concentrated under rotary evaporator to give desired compound.

Chemical Formula (a3): C₁₃H₁₉N₃O₈; 80% Yield, The IR spectrum showed the absence of azide absorption band of starting in ν (2101cm⁻¹).

Chemical Formula (b3): C₁₆H₂₃N₃O₁₀; yellow powder; 80% Yield, The IR spectrum showed the absence of azide absorption band of starting in ν (2102cm⁻¹).

5- General Synthesis of 1,2,3-triazole derivatives (a5)&(b4)¹⁷.

To a solution (0.01 mol) of compound a4 &b3 in (30 mL) of DMSO, (0.01 mol) of azide derivatives was added. After the mixture showed a homogeneity, sodium ascorbate (0.35 g, 1.78 mmol) and cuprous chloride (0.17 g, 1.78 mol) were added and the mixture was stirred at 60 CO for 72 hrs. The reaction course was followed by TLC ethyl acetate: hexane (1:1) as eluent. The crude material was purified by column chromatography-ethyl acetate: hexane (1:1) and concentrated under rotary evaporator to give desired compound a5&b4.

Chemical Formula a5: C₂₄H₂₅N₃O₁₁, 80% Yield; FTIR, disappearance of azide and appearance 3129, 2924, 2857,1713, 1618, cm⁻¹; ¹H NMR (500 MHz, Chloroform-d) δ 7.88 – 7.82 (m, 2H), 7.73 (d, J = 8.3 Hz, 3H), 7.54 (s,1H triazole), 7.37 – 7.19 (m, 5H), 5.83 (dd, J = 8.3, 4.2 Hz, 2H), 5.47 (tt, J = 11.5, 5.6 Hz, 2H), 5.39 – 5.31 (m, 4H), 4.92 – 4.82 (m, 3H), 4.80 (dt, J = 8.0, 3.9 Hz, 1H), 4.63 (t, J = 11.4 Hz, 2H), 4.42 (dt, J = 15.1, 7.6 Hz, 2H), 4.19 (s, 2H), 3.09 (td, J = 7.6, 7.0, 4.4 Hz, 6H), 2.42 (dd, J = 8.7, 4.2 Hz, 1H), 2.19 – 1.91 (m, 17H), 1.43 – 1.36 (m, 1H), 1.32 – 1.17 (m, 9H).

¹³C NMR (126 MHz, Chloroform-d) δ 169.59 (d, J = 33.0 Hz), 164.44, 162.09, 152.88, 132.16, 129.52, 127.37, 124.59, 123.50, 122.58, 116.36, 114.96, 96.22, 90.77, 70.17, 69.46, 69.14, 67.29, 62.19, 54.97, 50.45, 29.24, 20.24.

Chemical Formula b4: - C₂₇H₂₉N₃O₁₃, 80% Yield, FTIR, disappearance of azide and appearance 3175, 2923, 2857,1712, 1625, cm⁻¹;

¹H NMR (500 MHz, Chloroform-d) δ 7.82 (s, 1H), 7.71 (s, 1H triazole), 7.53 (s, 2H), 7.25 (d, J = 11.8 Hz, 2H), 5.33 (s, 1H), 5.17 (s, 1H), 5.07 (s, 1H), 5.00 (s, 3H), 4.62 (s, 2H), 4.50 (s, 1H), 4.23 (s, 4H), 4.13 (s, 2H), 3.96 (s, 2H), 3.70 (s, 2H), 2.99 (s, 1H), 2.33 (s, 1H), 2.07 (t, J = 9.3 Hz, 5H), 2.04 – 1.95 (m, 12H of 3CH₃).

Removal of protective groups Synthesis of (a6,b5)¹⁸

Compounds (0.3 mmol), were dissolved in methanol (5 mL), sodium ethoxide (2.04 mg, 0.03 mmol) was added thereto. Then the reaction mixture was stirred at room temperature until disappearance of starting material (6 hours) and concentrated. Then it was extracted with 40 mL of diethyl ether three times and then the organic phase was treated with 100 mL of water (three times). Subsequently, the diethyl ether phase was dried by adding anhydrous sodium sulfate (Na₂SO₄) and then filtered. The diethyl ether was evaporated and then the residue was dried.

4-((1-(((2R,3S,4S,5R,6R)-3,4,5-trihydroxy-6-methoxytetrahydro-2H-pyran-2-yl) methyl)-114,212,3-triazol-4-yl) oxy)-2H-pyran-2-one (a6)
Chemical Formula: C₁₈H₁₉N₃O₈, 88% Yield;
FTIR, 3394, 2924, 2857, 1709, 1615, cm⁻¹.

¹H NMR (500 MHz, DMSO-d₆) δ 7.78 (s, 1H triazole), 7.67 – 7.60 (m, 1H), 7.41 – 7.29 (m, 2H), 5.87 (d, J = 11.8 Hz, 1H), 5.16 (s, 1H), 4.46 (s, 2H), 3.98 (d, J = 5.0 Hz, 2H), 3.65 (s, 1H), 2.95 (d, J = 5.8 Hz, 1H), 2.45 (s, 1H), 1.20 (s, 4H).

4-((1-(2-(((2R,3R,4S,5S,6R)-3,4,5-trihydroxy-6-(hydroxy methyl) tetrahydro-2H-pyran-2-yl) oxy) ethyl)-114,212,3-triazol-4-yl) oxy)-2H-chromen-2-one (b5).

Chemical Formula: C₁₉H₂₁N₃O₉, 88% yield,
FTIR, 3409, 3187, 2923, 2857, 1712, 1625, cm⁻¹.

2.2 Molecular docking studies

Docking studies of the significantly active and weakly active compounds were performed using Glide module¹⁹ of Schrodinger software²⁰ installed on Intel Xenon W 3565 processor and

Ubuntu enterprise version 14.04 as an operating system. The selected target protein structure was retrieved from RCSB protein data bank²¹. Targeted ligands were drawn using Chemdraw 18.0 Perkinelmer software.

2.2.1. Ligand preparation

The ligands used as an input for docking study was sketched by ChemDraw software and cleaned up the structure for bond alignment. Then, ligands were incorporated into the workstation and the energy was minimized using OPLS3e (Optimized Potentials for Liquid Simulations)²² force field in Ligprep²³ (Version 2019-1, Schrodinger). This minimization helps to assign bond orders, the addition of hydrogens to the ligands and conversion of 2D to 3D structure for the docking studies. The generated output file (Best conformations of the ligands) was further used for docking studies.

2.2.2. Protein preparation

Protein preparation wizard²⁴ (Version 2019-1, Schrodinger) was the main tool in Schrodinger to prepare the protein and minimizing the protein. Hydrogen atom was added to the protein and charges were assigned. Generated Het states using Epik at pH 7.0 \pm 2.0. Preprocess the protein and refine, modify the protein by analyzing the workspace water molecules and other. The critical water molecules remained the same and rest of the molecules apart heteroatoms from the water was deleted. Finally, the protein was minimized using OPLS3 force field. A grid was created by considering co-crystal ligand, which was included in the active site of the protein of the selected target (PDB-4GQR). After the final step of docking with the co-crystal ligand in XP mode, root mean square deviation (RMSD) was checked to validate the protein, and the RMSD value lies within the range of 0.46 Å.

2.2.3. Receptor grid generation

A receptor grid was generated around the protein (PDB:4GQR)²⁵ by choosing the inhibitory ligand (X-ray pose of the ligand in the protein). The centroid of the ligand was selected to create a grid

box around it and Vander Waal radius of receptor atoms was scaled to 1.00 Å with a partial atomic charge of 0.25.

2.2.4. Docking and analysis

Molecular docking was performed using the above prepared ligand and protein as input. The results of the docking study were analyzed with the help of XP Visualizer (Version 2019- 1, Schrodinger). SMILES format of the compounds was generated by using OSIRIS Data warrior 26. Docking studies of the designed and synthesized molecules were performed by using Glide module in Schrodinger. All docking calculations were performed using Extra Precision (XP) mode. A scaling factor of 0.8 and a partial atomic charge of less than 0.15 was applied to the atoms of the protein. Glide docking score was used to determine the best docked confirmation from the output. The interactions of these docked conformations were investigated further using XP visualizer.

2.3. Biological Evaluation

Cytotoxic Screening

Preparation Primary Cell culture of true cut Breast tumor biopsies

The following protocol has been contributed by V.Speirs, Breast Research Group, Leeds Institute of Molecular Medicine, St James's University Hospital, Leeds LS9 7TF, UK, adapted from Speirs (2004). The true-cut biopsies of the patients were obtained by the oncologist with assistance from a radiologist from the breast tumor under local anesthesia and assisted by ultrasound imaging; then transferred to the cell culture unit.

Preparation Primary Cell culture of true cut Liver and tumor biopsies

The true cut biopsies of the patients were obtained by oncologist from the core of liver cancer under local anesthesia and assisted by ultrasound imaging; then transferred to the cell transplant unit²⁷.

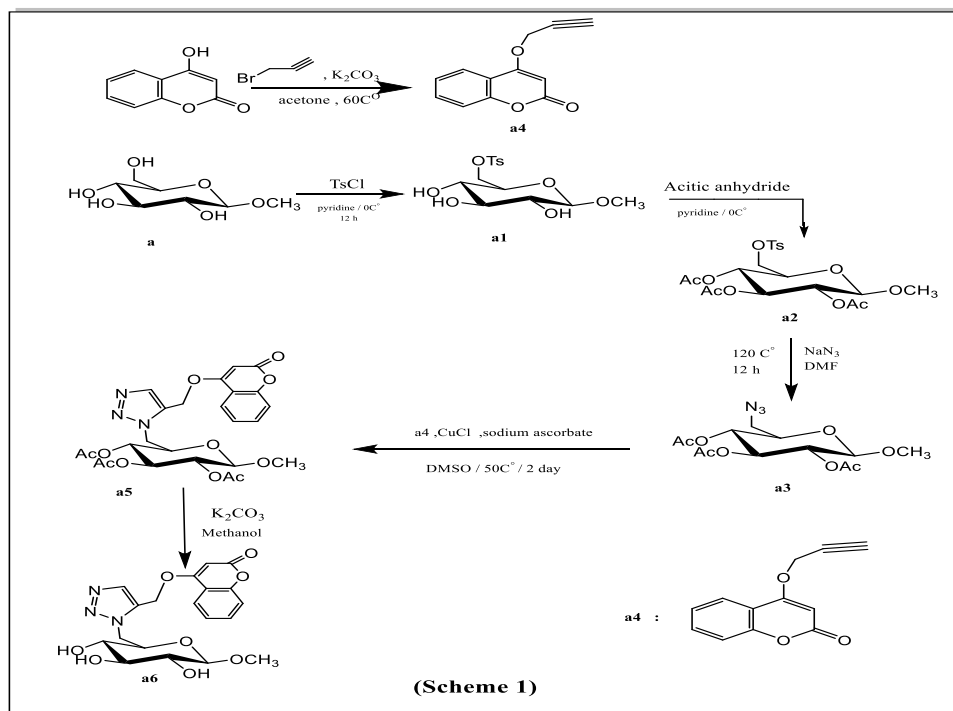
Cell Cytotoxicity determination using MTT assay

This assay done according to Briefly²⁸, cells were seeded at 1×10^5 cells/mL in 96 well micro titer plates containing DMEM medium with supplement. Fifty μ l with different concentrations of b5 (500,100,50,25,12.5) μ g/ ml and b5. (20,100, 200,1000) μ g/ ml were diluted in media and added in triplicate, control cells received only serum free media, incubated for 24 hrs. Thereafter, the cells were treated with 30 μ l of MTT (3-(4,5-Dimethyl-2-thiazolyl)-2,5-diphenyl-2H-tetrazolium bromide) at concentration 2 μ g/ml for 1hr. After the incubation time (37° C, 5 % CO₂). 30 μ l DMSO (Dimethyl sulfoxide) 1% was added to each well then incubate in the dark condition for 30 min at the room temperature, then measured the absorbance at 630 nm using microplate reader²⁹

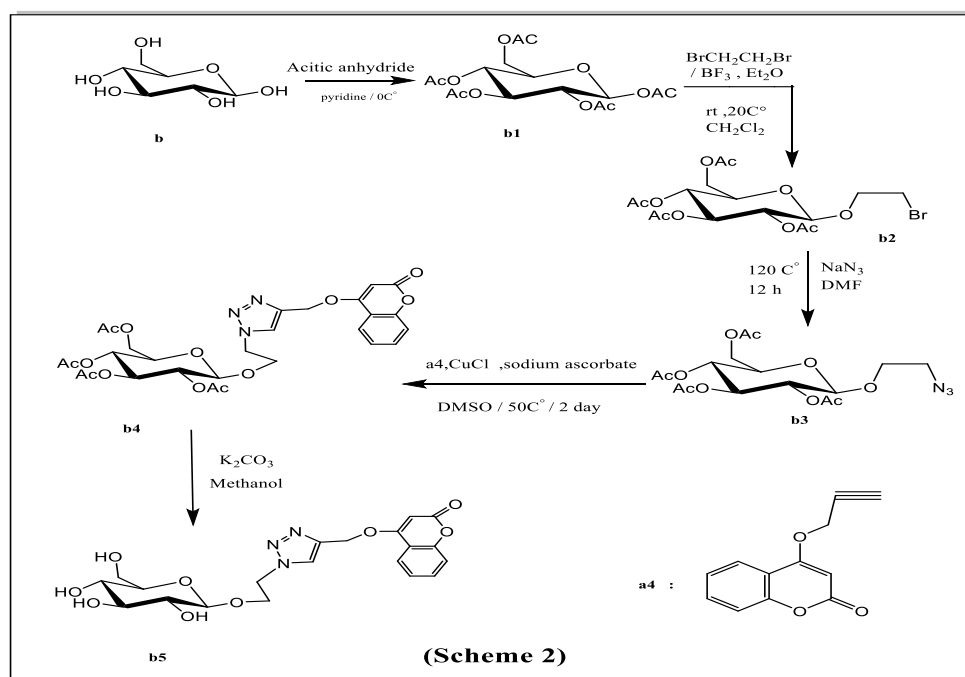
3 RESULTS AND DISCUSSION

The unique bands of the azide group may be seen in the infrared spectra of the azide product. the triplet signals of the methylene groups in the side-chain substituent linked to the glucose ring were visible in the matching ¹H NMR spectra. By use of a Cu-catalyzed cycloaddition reaction (CuCAAC), the synthesized azide a3 and b3 were combined with the propargyl 4-hydroxy coumarin under click circumstances to create the 1,2,3-triazole glycosides. The necessary Cu(I) catalyst was produced using copper sulfate and sodium ascorbate by in-situ reducing copper (II) in the reaction solution. Following the evaluation of various solvent systems, it was found that DMSO was the most effective solvent and produced the desired 1,2,3-triazole compounds. Follows the development of the interaction by TLC. The yields were less than 52% after 2 days and 55 hours of stirring at 60 °C, respectively. Glycosides in the latter structures. At their known assigned values, the IR spectra of compounds a2 and b3 showed distinctive bands connected to the carbonyl frequency in the acetate group. The coupling constant of the anomeric proton in their ¹H NMR spectra revealed signals ascribed to the sugar fragments, which were allocated to the produced -confirmation of the triazole-sugar bond. Under the influence of a saturated

ammonia solution in methanol, the acetylated glycosides a5 and b4 underwent a deprotection reaction that produced the triazole glycosides a6 and b5 with free hydroxyl groups, which was consistent with their spectral data (Scheme 1).



Other functionalized azide compounds, a3 and b3, were also synthesized using the click method. As a result, the reaction was carried out in this manner to achieve the connection of the terminal 4-hydroxy coumarin with azide sugar to produce the 1,2,3-triazole glycosides.



3.1. Biological Evaluation

Determine the cell cytotoxicity by using MTT assay

Determine the anticancer activity of b5 against liver carcinoma.

The cytotoxicity potentials of b5 were evaluated

by MTT assay against liver cancer primary tissue culture after 48 hr., which appear that b5 exhibited selective cytotoxicity against liver cancer cells isolated from Iraqi patients with inhibitory concentration (IC₅₀) 106.81 µg/ml as showed in figure (1) and table (1).

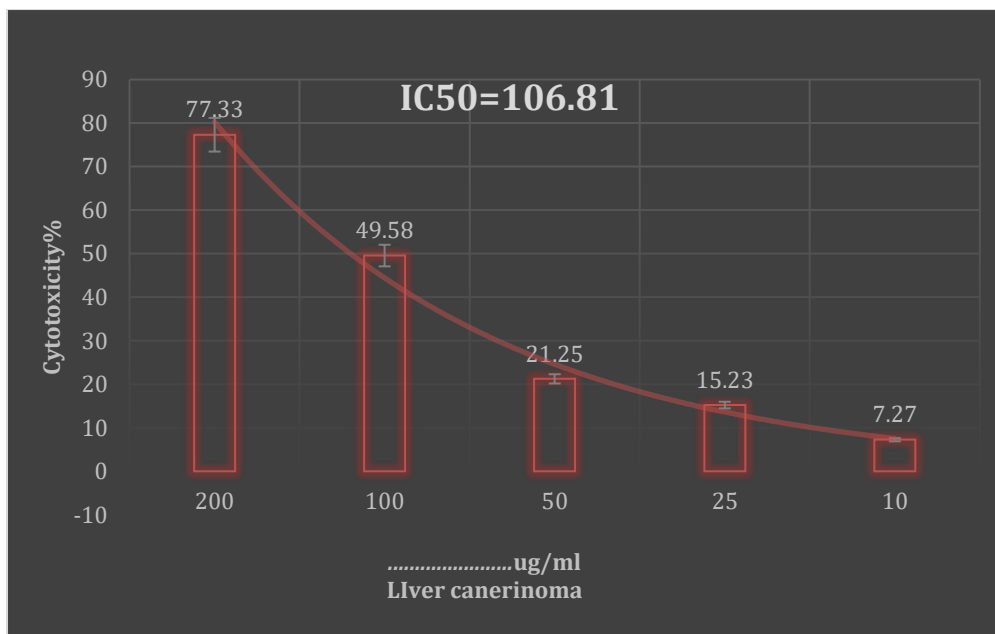


FIGURE 1: The cytotoxic effect of b5 against Human liver cancer cells after 48 hrs. of exposure.

TABLE 1: The equation form to calculate the IC₅₀ of b5 against liver cancer cells isolated from Iraqi patients by using AAT Bio-quest website

IC ₅₀ Regression Results [Dataset 1]	
Parameter	Value
IC ₅₀	106.8176
Equations	
Equation	$Y = 4.3111 + \frac{91.5602 - 4.3111}{1 + \left(\frac{X}{106.8176}\right)^{2.124}}$
Equation Form	$Y = \text{Min} + \frac{\text{Max} - \text{Min}}{1 + \left(\frac{X}{\text{IC}_{50}}\right)^{\text{Hill coefficient}}}$

The determination the effect of b5 on Apoptosis (DNA Fragmentation) by Using Acridine-Orange / Ethidium Bromide (AO/EB) Technique.

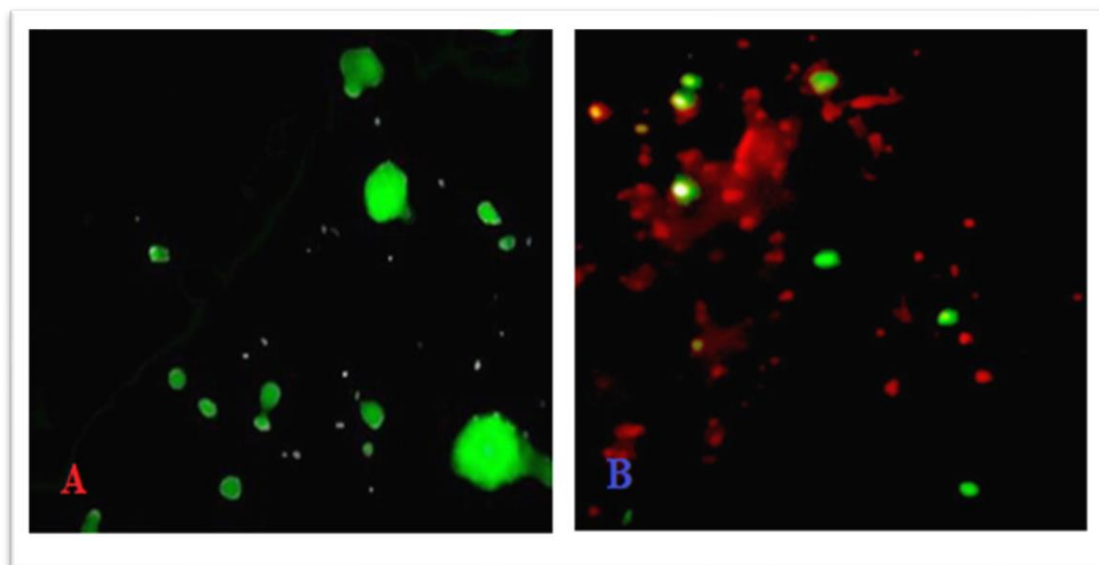


FIGURE 2: The fluorescence microscope image to primary cell culture of human liver cancer cells stained with AO / EtBr and represent the apoptosis method. (A) Untreated liver cancer cells (100x), (B) liver cancer cells treated with b5 with 200ug/ml after 48 h (100 x)

3.2. Molecular Docking Study

The Molecular Operating Environment (MOE-Dock) software version 2014.0901 was used to do docking simulations for targets a5, a6, b4, and b5 in order to evaluate their promising in vitro inhibitory effects and comprehend their binding mechanisms within the EGFRWT, EGFR790M, and HER-2 active sites. The Protein Data Bank files for the relevant EGFRWT, EGFR790M, and HER-2 enzymes (PDB codes: 1M17, 3UG2, and 3RCD, respectively) were selected and downloaded³⁰.

Selection of protein crystal structures

Crystallographic structures of Protein: - Mitogen-activated protein kinase (JNK1) are provided in the Protein Data Bank pdb code (A1 chain with) (4AWI). This section evaluates and chooses the 4AWI crystal structure for docking³¹. The MOE structure organization technique corrected the faults in the protein by identifying the biggest and ligand pockets, inserting the tested compounds in these pockets for docking, ligand interaction, computing the total binding energy, and calculating the H-bond and Van der Waals (VDW) energies.

Ligand Interactions Report Compound (a5)

Ligand	Receptor	Interaction	Distance	E(kcal/mol)
C 43	5-ring HIS	66 (A) H-pi	4.75	-1.0
6-ring	CA GLY	33 (A) pi-H	3.55	-1.4

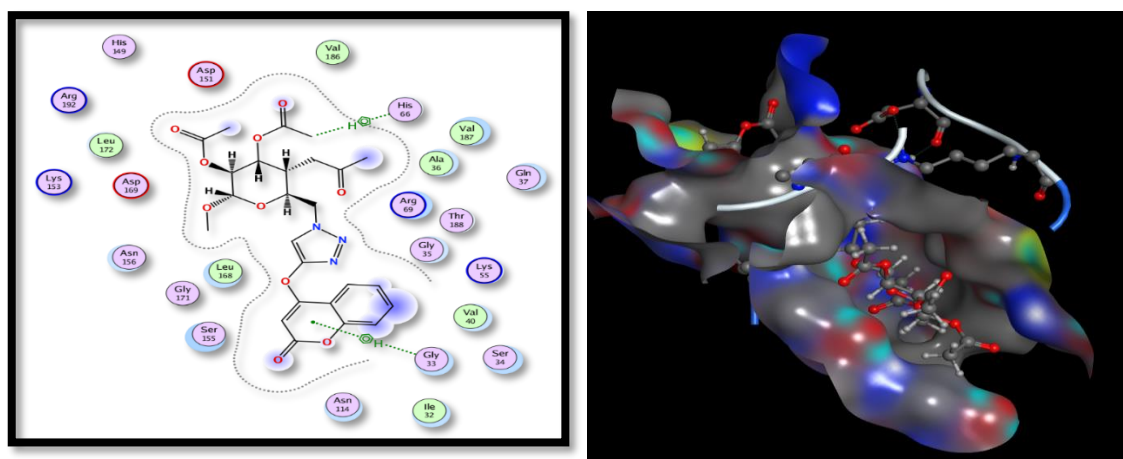


FIGURE 3: Two-dimensional views of compounds a5, respectively, docked in the active binding site of EGFRT790M (PDB ID: 3UG2) using MOE software

Ligand Interactions Report a6

4AWI: TRANSFERASE / 4AWI

Ligand	Receptor	Interaction	Distance	E (kcal/mol)
O 41	NH2 ARG 192	(A) H-acceptor	2.80	-1.2
5-ring	NZ LYS 153	(A) pi-cation	4.28	-1.5
6-ring	NH2 ARG 192	(A) pi-cation	4.18	-1.3

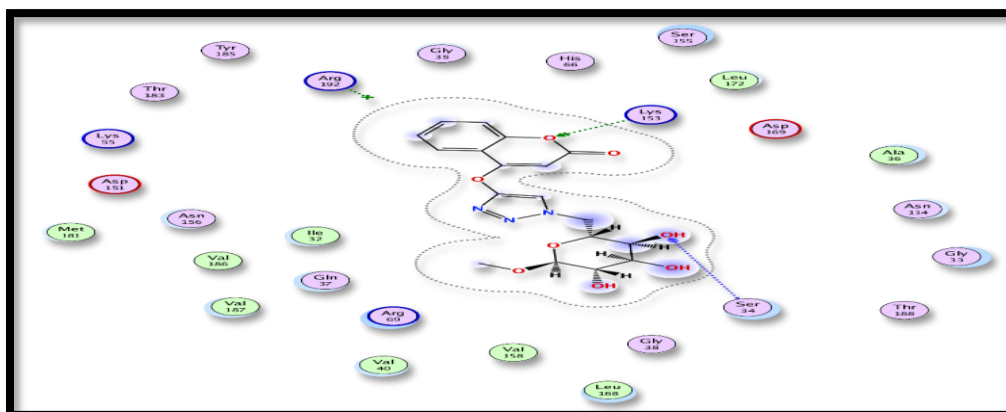


FIGURE 4: Two-dimensional views of compounds a6, respectively, docked in the active binding site of EGFRT790M (PDB ID: 3UG2) using MOE software

Ligand Interactions Report b4

4AWI: TRANSFERASE / 4AWI

Ligand	Receptor	Interaction	Distance	E (kcal/mol)
C 43	O SER 34 (A)	H-donor	3.40	-0.7
N 23	N THR 188 (A)	H-acceptor	3.11	-1.1
5-ring	CG1 VAL 186 (A)	pi-H	4.25	-0.6

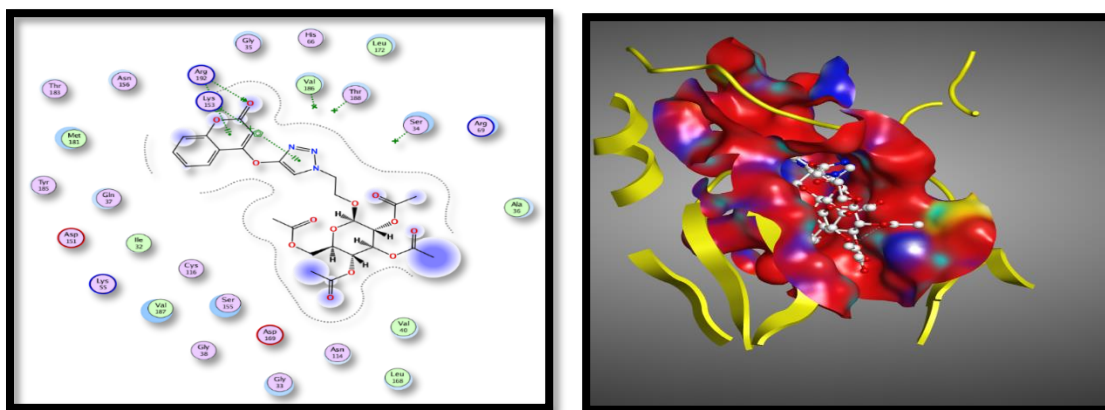


FIGURE 5: Two-dimensional views of compounds b4, respectively, docked in the active binding site of EGFRT790M (PDB ID: 3UG2) using MOE software.

Ligand Interactions Report b5

4AWI: TRANSFERASE / 4AWI

Ligand	Receptor	Interaction	Distance	E (kcal/mol)
O 8	N SER 34 (A)	H-acceptor	3.03	-1.3
O 31	NZ LYS 153 (A)	H-acceptor	3.13	-0.8

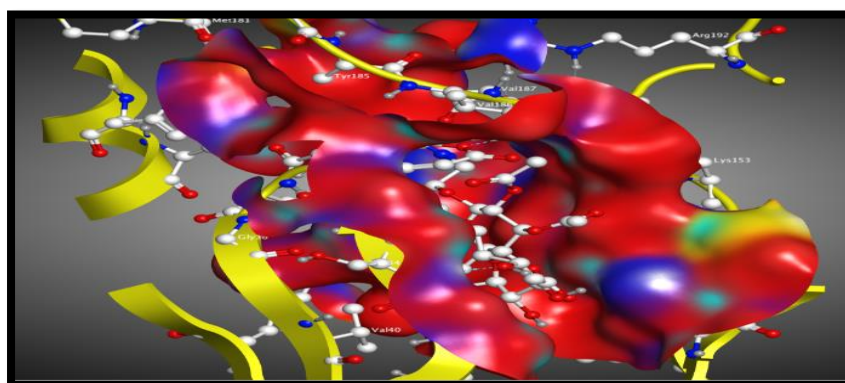


FIGURE 6: Two-dimensional views of compounds b5, respectively, docked in the active binding site of EGFRT790M (PDB ID: 3UG2) using MOE software

Regarding the EGFRWT receptor, the triazole fragments in (a5) were observed to play a vital role in binding through arene–arene interactions with amino acid His66. The essential amino acid Glu33 exhibited arene–cation interactions with p-tolyl and with coumarin ring in triazole derivatives (Figure 3). Within EGFRT790M (Figure 4), arene–cation interactions were illustrated between Arg 192 and the p-tolyl and

Gln37 and the glucose ring in compound a6.

While, the compound b4, b5 was observed to play a vital role in binding through arene–arene interactions with amino acid Arg192, lys253, in b5 and the amino acid lys153 and ser 34 in b5 exhibited arene–cation interactions with p-tolyl and with coumarin ring in triazole derivatives observe in Figure (4&5)

4. CONCLUSIONS

A series of new coumarin derivatives containing heterocyclic with mono saccharide derivatives. The synthesized compound b5 showed excellent anti-cancer activity.

REFERENCES

1. A. Zorin, L. Klenk, T. Mack, H.P. Deigner, and M. S. Schmidt, "Current Synthetic Approaches to the Synthesis of Carbasugars from Non-Carbohydrate Sources, *Top. Curr. Chem.*, 2022, 380, 2, pp. 1–31.
2. A. F. Razaq and M. J. Mohammed, "Synthesis and Studying of the Biological Activity of Some New Coumarin-3-carboxylic Acid Heterocyclic Derivatives, *Egypt. J. Chem.*, 2022, 65, 2, pp. 35–40.
3. M. M. Heravi, S. Khaghaninejad, and M. Mostofi, Pechmann reaction in the synthesis of coumarin derivatives," in *Advances in heterocyclic chemistry*, 2014, 112, Elsevier, , pp. 1–50.
4. M. Tolba et al., "An overview on synthesis and reactions of coumarin based compounds, *Curr. Chem. Lett.*, 2022, 11, 1, pp. 29–42.
5. A. S. Barrow, C. J. Smedley, Q. Zheng, S. Li, J. Dong, and J. E. Moses, The growing applications of SuFEx click chemistry," *Chem. Soc. Rev.*, 2019, 48, 17, pp. 4731–4758.
6. S. I. Presolski, V. P. Hong, and M. G. Finn, Copper-catalyzed azide–alkyne click chemistry for bioconjugation," *Curr. Protoc. Chem. Biol.*, 2011, 3, 4, pp. 153–162.
7. Y. Shi, X. Cao, and H. Gao, "The use of azide–alkyne click chemistry in recent syntheses and applications of polytriazole-based nanostructured polymers, *Nanoscale*, 2016, 8, 9, pp. 4864–4881.
8. M. S. Singh, S. Chowdhury, and S. Koley, "Advances of azide-alkyne cycloaddition-click chemistry over the recent decade , *Tetrahedron*, 2016, 72, 35, pp. 5257-5283
9. E. Bonandi, M. S. Christodoulou, G. Fumagalli, D. Perdicchia, G. Rastelli, and D. Passarella, "The 1, 2, 3-triazole ring as a bioisostere in medicinal chemistry, *Drug Discov. Today*, 2017, 22, 10, pp. 1572–1581.
10. F. Wei, W. Wang, Y. Ma, C.-H. Tung, and Z. Xu, "Regioselective synthesis of multisubstituted 1, 2, 3-triazoles: moving beyond the copper-catalyzed azide–alkyne cycloaddition, *Chem. Commun.*, 2016, 52, 99, pp. 14188–14199..
11. R. S. Gomes, G. A. M. Jardim, R. L. de Carvalho, M. H. Araujo, and E. N. da Silva Júnior, "Beyond copper-catalyzed azide-alkyne 1, 3-dipolar cycloaddition: Synthesis and mechanism insights, *Tetrahedron*, 2019, 75, 27, pp. 3697–3712.
12. J. El-Abid, V. Moreau, J. Kovensky, and V. Chagnault, "Effects of CoCl₂ on the regioselective tosylation of oligosaccharides, *J. Mol. Struct.*, 2021, 1241, p. 130609.
13. V. Yarlagadda, M. M. Konai, G. B. Manjunath, C. Ghosh, and J. Haldar, "Tackling vancomycin-resistant bacteria with 'lipophilic–vancomycin–carbohydrate conjugates, *J. Antibiot. (Tokyo)*. 2015. 68, 5, pp. 302–312.
14. Z. D. Wang, Y. Mo, C.-L. Chiou, and M. Liu, "A simple preparation of 2, 3, 4, 6-tetra-O-acyl-gluco-, galacto-and mannopyranoses and relevant theoretical study, *Molecules*, 2010. 15, 1, pp. 374–384.
15. M. M. Zeydi, S. J. Kalantarian, and Z. Kazeminejad, "Overview on developed synthesis procedures of coumarin heterocycles, *J. Iran. Chem. Soc.*, 2020., 17, 12, pp. 3031–3094.
16. S. Hao et al., "Design, synthesis and biological evaluation of novel carbohydrate-based sulfonamide derivatives as antitumor agents, *Bioorg. Chem.*, 2020, 104, p. 104237.
17. V. Aragão-Leoneti, V. L. Campo, A. S. Gomes, R. A. Field, and I. Carvalho, "Application of copper (I)-catalysed azide/alkyne cycloaddition (CuAAC)'click chemistry' in carbohydrate drug and neoglycopolymer synthesis, *Tetrahedron*, 2010. 66, 49, pp. 9475–9492.
18. A. I. Mohammed, N. H. Mansour, and L. S. Mahdi, "Synthesis and antibacterial activity of 1-N-(β-d-glucopyranosyl)-4-((1-substituted-1H-1, 2, 3-triazol-4-yl) ethoxymethyl)-1, 2, 3-triazoles, *Arab. J. Chem.*, 2017. 10, pp. S3508–S3514.
19. R. A. Friesner et al., "Glide: a new approach for rapid, accurate docking and scoring. 1. Method and assessment of docking accuracy, *J. Med. Chem.*, 2004. 47, 7, pp. 1739–1749.
20. S. Release, "1: Maestro, Schrodinger, 2019 LLC, New York..
21. S. K. Burley et al., "RCSB Protein Data Bank: biological macromolecular structures enabling research and education in fundamental biology, biomedicine, biotechnology and energy, *Nucleic Acids Res.*, 2019, 47, D1, pp. D464–D474.
22. W. L. Jorgensen, D. S. Maxwell, and J. Tirado-Rives, "Development and testing of the OPLS all-atom force field on conformational energetics and properties of organic liquids, *J. Am. Chem. Soc.*, 1996. 118, 45, pp. 11225–11236.
23. S. Release, "4: LigPrep, Schrödinger, 2019.LLC, New York, NY.
24. A. C. Kaushik, D. Gautam, A. S. Nangraj, D.-Q. Wei, and S. Sahi, "Protection of primary

- dopaminergic midbrain neurons through impact of small molecules using virtual screening of gpr139 supported by molecular dynamic simulation and systems biology, *Interdiscip. Sci. Comput. Life Sci.*, 2019. 11, 2, pp. 247–257.
25. L. K. Williams, C. Li, S. G. Withers, and G. D. Brayer, “Order and disorder: differential structural impacts of myricetin and ethyl caffeate on human amylase, an antidiabetic target, *J. Med. Chem.*, 2012, 55, 22, pp. 10177–10186.
 26. T. Sander, J. Freyss, M. von Korff, and C. Rufener, “DataWarrior: an open-source program for chemistry aware data visualization and analysis, *J. Chem. Inf. Model.*, 2015. 55, 2, pp. 460–473.
 27. C.-F. Liu, Q.-K. Shen, J.-J. Li, Y.-S. Tian, and Z. Quan, “Synthesis and biological evaluation of novel 7-hydroxy-4-phenylchromen-2-one-linked to triazole moieties as potent cytotoxic agents, *J. Enzyme Inhib. Med. Chem.*, 2017. 32, 1, pp. 1111–1119.
 28. T. Hayon, A. Dvilansky, O. Shpilberg, and I. Nathan, “Appraisal of the MTT-based assay as a useful tool for predicting drug chemosensitivity in leukemia, *Leuk. Lymphoma*, 2003, 44, 11, pp. 1957–1962.
 29. S. Kasibhatla, G. P. Amarante-Mendes, D. Finucane, T. Brunner, E. Bossy-Wetzel, and D. R. Green, “Acridine orange/ethidium bromide (AO/EB) staining to detect apoptosis,” *Cold Spring Harb. Protoc.*, 2006, 3, p. 4493..
 30. H. E. Hashem, A. E.-G. E. Amr, E. S. Nossier, M. M. Anwar, and E. M. Azmy, “New benzimidazole-, 1, 2, 4-triazole-, and 1, 3, 5-triazine-based derivatives as potential EGFRWT and EGFR790M inhibitors: microwave-assisted synthesis, anticancer evaluation, and molecular docking study, *ACS omega*, 2022, 7, 8, pp. 7155–7171.
 31. H. S. Mohammed, S. William, T. Aboushousha, H. M. A. Taleb, R. Sabour, and M. A. Ghareeb, “*Ailanthus excelsa* leaf extract: Chemical characterization, antischistosomal activity, and in silico study of isolated phenolic compounds as promising thioredoxin glutathione reductase inhibitors, *J. Appl. Pharm. Sci.*, 2023,13, 2, pp. 124–145.